Magnetic and Magnetocaloric Effect of Laves Phase Compounds Er(Fe0.8–xMn0.2–yCox+y)2 with x, y = 0.0 or 0.1

Safa Othmani, Ichrak Chaaba, Sonia Haj-Khlifa, Patricia de Rango, Daniel Fruchart

metals

MDPI

Article

Magnetic and Magnetocaloric Effect of Laves Phase Compounds $Er(Fe_{0.8-x}Mn_{0.2-y}Co_{x+y})_2$ with x, y = 0.0 or 0.1

Safa Othmani [1], Ichrak Chaaba [2], Sonia Haj-Khlifa [3], Patricia de Rango [3] and Daniel Fruchart [3,*]

[1] Unité de Recherche sur les Hétéro-Epitaxies et Applications, Faculté des Sciences de Monastir 5019, Université de Monastir, Monastir 5000, Tunisia; safa.othmani@gmail.com

[2] Laboratoire des Technologies des Systèmes Smart, C.R.I. Multimédia et Traitement Numérique des Données, Technopôle de Sfax, B.P 275, Sfax 3029, Tunisia; chishrak@hotmail.fr

[3] Institut Néel & Université Grenoble Alpes, B.P. 166, 38042 Grenoble CEDEX 9, France; soniahajkhlifa@gmail.com (S.H.-K.); patricia.derango@neel.cnrs.fr (P.d.R.)

* Correspondence: daniel.fruchart@neel.cnrs.fr; Tel.: +33-607268991

Received: 5 August 2020; Accepted: 7 September 2020; Published: 16 September 2020

Abstract: Magnetic and magnetocaloric effect (MCE) of the $Er(Fe_{0.8-x}Mn_{0.2-y}Co_{x+y})_2$ Laves phase-type compounds have been investigated. X-ray diffraction (XRD) analysis has revealed that these compounds crystallize with the C15 type Laves phase structure (Space Group *Fd-3m*). The magnetization curves indicate a ferri-magnetic-ordering resulting of the antiparallel coupling between the moments of the heavy rare earth Er and the transition metal (TM). The partial substitution of Fe/Mn by Co increases the Curie temperature from 355 K for $Er(Fe_{0.8}Mn_{0.2})_2$ to 475, 550, and 555 K for $Er(Fe_{0.7}Mn_{0.2}Co_{0.1})_2$, $Er(Fe_{0.8}Mn_{0.1}Co_{0.1})_2$, and $Er(Fe_{0.7}Mn_{0.1}Co_{0.2})_2$, respectively. According to the nature of the TM elements, arguments were presented forwards either Molecular Field or Spin Fluctuation Theory, even Stoner type pictures should be considered for. MCE was calculated according to the Maxwell relation based on isotherm magnetization measurements. The magnetic entropy change ($-\Delta S_M$) observed on a 300–400 K temperature range can be understood in terms of a Spin Fluctuation Theory picture supported by both the different magnetic polarization levels that were shared by the TM elements and the related interatomic exchange forces.

Keywords: $R(TM)_2$ compounds; X-Ray diffraction; magnetic properties; magnetocaloric effect

1. Introduction

Magnetocaloric effect (MCE), which is considered as a foundation for the development of magnetic refrigeration, has attracted considerable attention during recent years [1–3]. Additionally, fundamental investigations of MCE phenomena reveal of high interest for a better knowledge of the local magnetic polarization, the exchange forces, and elastic couplings with the lattice [4,5]. Generally speaking, the MCE is characterized by determining both the isothermal magnetic entropy change (ΔS) and the adiabatic temperature change (ΔT_{ad}) of a material when exposed to a variation magnetic field. Most of the investigations on the MCE materials have focused on temperature ranges where occurs either a first order or a second order phase transition [1–6]. Usually, for the first order magnetic phase transition materials, large ΔS may be obtained in the vicinity of the magnetic transition temperature, owing to a sharp change of magnetization [1–4,6–12]. Accordingly, considerable attention has been paid to that type of materials for the development of efficient magnetic refrigeration systems, as was corroborated by early results. However, magnetic phenomena that may hinder the MCE yield narrow the magnetic refrigeration application of first order transition materials [12–14]. Besides, no magnetic/thermal hysteresis occurs along a wider temperature range, thus making the second

order transition materials attracting to investigate as well [14]. In fact, quite different series of high performance MCE materials were extensively considered for their fundamental properties as well for potential applications, e.g., in [1–19]. Among such series, magnetic Laves phases $R(Fe_{1-x}TM_x)_2$-type compounds, where R is a heavy rare earth metal sharing a high magnetic moment and transition metal (TM) is a magnetic transition metal, have retained our attention. The synthesis procedures and structural aspects remain rather simple comparison made with other types of compounds. In addition, the magnetic and electronic properties reveal particularly flexible in terms of saturation magnetization, ordering temperature, and type of transition order. The RFe_2 series exhibit ferri-magnetic arrangements with rather high ordering temperatures (second order type) and compensation points when $M_R(T) = -M_{TM}(T)$ [20–23]. Interestingly, in the RCo_2 binaries, the magnetic polarization on Co is typically driven by its itinerant electron character leading to rather low ordering temperature that was reported being of first order type [15]. The substitution of Fe to Co was expected, extending enough the ordering temperature towards room temperature, with the potential benefit of rather large variations of magnetic entropy (S) at the transition [24–27]. In order to lower and adjust the Curie temperature, even to suppress the compensation point, we have investigated the $Er(Fe_{1-x}Co_x)_2$ and $R(Fe_{1-x}Co_x)_2H_y$ hydrides with R = Ho, Er for their magnetic and magnetocaloric properties, as shown in ref. [28,29]. For all cases, a rather flat magnetic entropy variation was revealed, extending on a large range of temperature (e.g., 100 to 400 K), which remains of limited intensity. However, a sharp and marked S signal was evidenced in the lowest temperature range for the hydrogenated compounds, similar to that found for the pure $ErCo_2$ binary [15].

Besides, investigations of $Er(Fe_{1-x}Mn_x)_2$ compounds revealed that substitutions of Fe by Mn lead to remarkable impacts on both crystal structure and magnetic properties, since manganese tends superimpose antiferromagnetic (AFM) TM-TM exchange couplings [30–32].

In the present work, we report on the structural, magnetic, and magnetocaloric properties of Co-substituted $Er(Fe_{0.8}Mn_{0.2})_2$ compounds. Small Mn contents only where chosen in order to maintain the cubic $MgCu_2$ (C15 type) structure. The counterbalance effects of Co to Mn were considered for, since Co favors ferromagnetic interactions in spite of sharing a low magnetic moment and Mn drives AFM exchange couplings with a possibly high magnetic moment. For this doing, the $Er(Fe_{0.8}Mn_{0.1}Co_{0.1})_2$, $Er(Fe_{0.7}Mn_{0.2}Co_{0.1})_2$, and $Er(Fe_{0.7}Mn_{0.2}Co_{0.2})_2$ compounds were synthesized, and their structure, magnetic, and magnetocaloric properties were analyzed.

2. Materials and Methods

All of the samples were prepared from high-purity elements Er(3N), Mn(4N), Fe(3N8), and Co(4N) using high frequency melting under purified Ar atmosphere (5 N). A small excess of Mn was added to the starting compositions to prevent any loss due to its high vapor pressure. The homogeneity of the ingots was insured with five successive melting procedures.

Systematic X-ray diffraction analyses were carried out at room temperature using a Siemens reflection diffractometer D5000R (Bruker AXS GmbH, Östliche Rheinbrückenstr. 49, 76187 Karlsruhe Germany) operating at $\lambda_{Co,K\alpha 1}$ wavelength.

Magnetization traces were recorded using the two extraction-type magnetometers developed at Institut Néel, respectively, for high temperature (300–900 K) and for low temperature (5–330 K) ranges. For the different compounds, the magnetic transition temperatures were determined by determining the position of the first derivative (dM/dT) peaks of traces recorded under a low magnetic field of 0.05 T. The magnetic entropy change S, which allows determine the MCE, was established using the Maxwell's relation from isothermal magnetization plots recorded versus magnetic field.

3. Results

3.1. Structure Analysis

Figure 1 shows the room temperature X-ray diffraction (XRD) patterns of $Er(Fe_{0.8-x}Mn_{0.2-y}Co_{x+y})_2$ (x, y = 0.0 or 0.1) compounds. Profile-type structure refinements were carried out using the Fullprof tool [33]. A single phase-material is observed for the substituted compounds without any impurity apart a tiny amount of Er_2O_3 for $Er(Fe_{1-x}Mn_x)_2$. All of the compounds were found crystallizing in the $MgCu_2$-type cubic Laves phase structure (C15-type, Space Group Fd-3m).

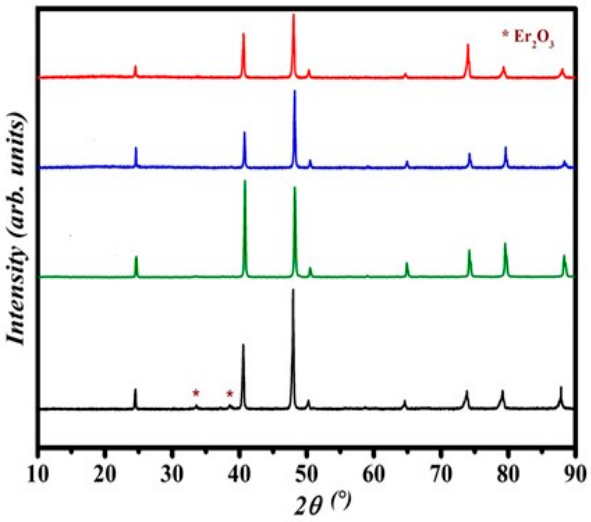

Figure 1. X-ray diffraction (XRD) patterns of $Er(Fe_{0.2}Mn_{0.8})_2$, (black), $Er(Fe_{0.8}Mn_{0.1}Co_{0.1})_2$ (green), $Er(Fe_{0.7}Mn_{0.2}Co_{0.1})_2$ (blue), and $Er(Fe_{0.7}Mn_{0.1}Co_{0.2})_2$ (red). A tiny amount of Er_2O_3 impurity was detected for $Er(Fe_{0.2}Mn_{0.8})_2$.

However, for $Er(Fe_{0.8}Mn_{0.2})_2$, very small additional peaks are notified, which may correspond to the erbium oxide (Er_2O_3), in amount not exceeding 3 mol.%. It may arise from the grinding of the ingot to fine powder needed for the XRD measurements. Figure 2 shows the indexation of patterns.

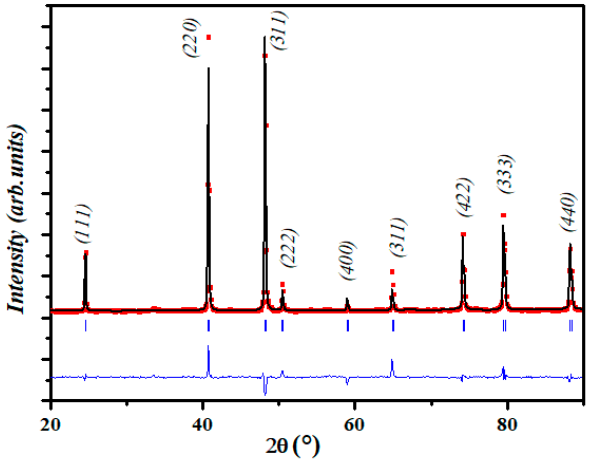

Figure 2. Observed (red) and calculated (black) XRD patterns of $Er(Fe_{0.8}Mn_{0.2}\ Co_{0.1})_2$. The difference pattern is plotted at the bottom. Bragg reflections are indicated by ticks.

For example, Figure 2 discloses the experimental XRD pattern of $Er(Fe_{0.8}Mn_{0.1}Co_{0.1})_2$ as compared with the calculated profile. Table 1 lists the refined cell parameters for all the studied compounds.

Please note that, for $Er(Fe_{0.8}Mn_{0.2})_2$, the present results fairly well agree with previously established data received on the $Er(Fe_{1-x}Mn_x)_2$ ($0 < x < 0.6$) system [31].

Table 1. Cell parameters at 300 K for $Er(Fe_{0.8}Mn_{0.2})_2$, $Er(Fe_{0.8}Co_{0.1}Mn_{0.1}\ Co_{0.1})_2$, $Er(Fe_{0.7}Mn_{0.2}\ Co_{0.1})_2$, and $Er(Fe_{0.7}Mn_{0.1}\ Co_{0.2})_2$ refined from XRD.

Compounds		Cell Parameter (Å)	Cell Volume (Å^3)
$Er(Fe_{0.8}Mn_{0.2})_2$	1	7.313(3)	391.18(3)
$Er(Fe_{0.8}Mn_{0.1}Co_{0.1})_2$	2	7.265(5)	383.54(2)
$Er(Fe_{0.7}Mn_{0.2}Co_{0.1})_2$	3	7.281(1)	386.02(1)
$Er(Fe_{0.7}Mn_{0.1}Co_{0.2})_2$	4	7.246(1)	380.42(2)

For the Co-substituted compounds, the unit-cell volume decreases comparison made to that of $Er(Fe_{0.8}Mn_{0.2})$, since the Co atomic radius is smaller than that of Fe and Mn with r_{Mn} = 1.61 Å, r_{Fe} = 1.56 Å, and r_{Co} = 1.52 Å, the calculated values accounting for the d-block contraction [34]. Accordingly, the Mn-richest compounds exhibit the largest unit cell volumes.

3.2. Magnetic Properties

Figure 3 shows the magnetization variation versus temperature of the $Er(Fe_{0.8-x}Mn_{0.2-y}Co_{x+y})_2$ compounds established in external magnetic field of 0.05 and 1 T.

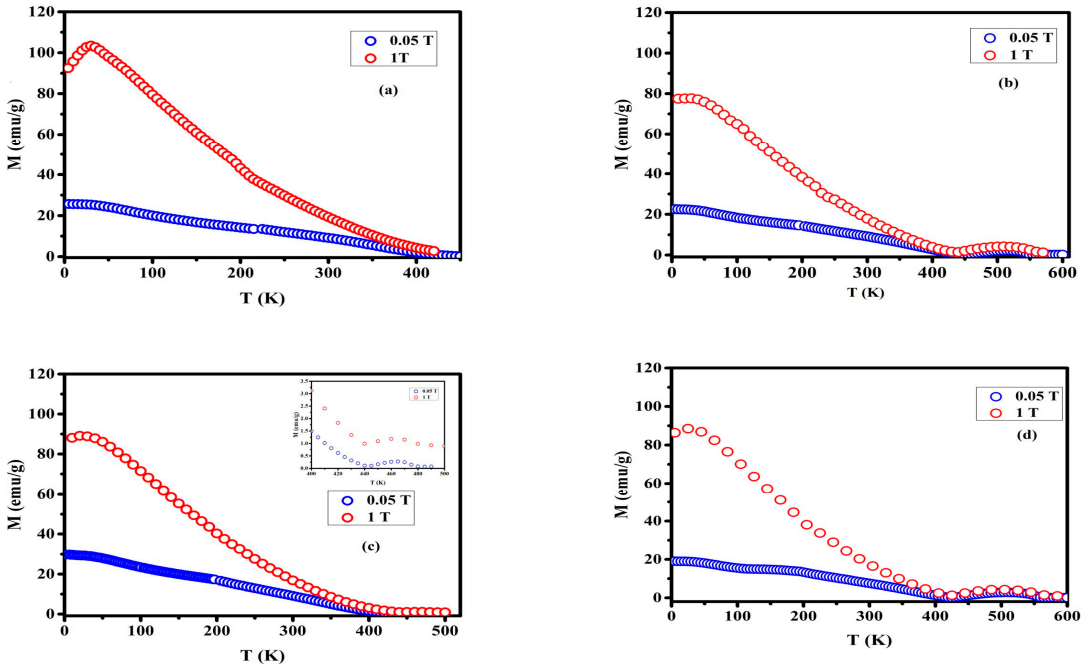

Figure 3. Temperature dependence of the magnetization under 0.05 T (blue) and 1 T (red) for (**a**) $Er(Fe_{0.8}Mn_{0.2})_2$ (**b**) $Er(Fe_{0.8}Mn_{0.1}Co_{0.1})_2$ (**c**) $Er(Fe_{0.7}Mn_{0.2}Co_{0.1})_2$ and (**d**) $Er(Fe_{0.7}Mn_{0.1}Co_{0.2})_2$. The inset of Figure 3 (**c**) allows distinguish in more details the magnetization behavior in between $T_{comp.}$ and T_C.

The M-T curves of all samples show smooth variations suggesting that the magnetic ordering transitions are of second order. However, the derivative trace reveals for all compounds a marked change of the susceptibility versus temperature nearby 50 K. This phenomenon should result of a differential thermal behavior of the anisotropy contribution of the erbium Crystal Electric Field (CEF) which was reported to increase at low temperature [35–37], whereas the molecular field addressed by the (Fe-TM) sublattice should be considered as almost unchanged [21,35–37].

All of the compounds are ferrimagnet (FI), according to the Russell–Saunders rules leading to antiparallel configurations between a TM(3d) moment and a heavy rare earth R(4f) moment via the R(5d)-TM(3d) overlapping orbitals. According to literature, the Er moment can be considered as fully saturated (~9 μ_B) [38–40], so being larger than twice the TM-3d one. At 355 K, $Er(Fe_{0.8}Mn_{0.2})_2$ exhibits a transition from ferri- (FI) to paramagnet (PM) states, as shown Figure 3a. In principle, the Er and TM magnetizations align antiparallel, but, when temperature increases high enough, the Er magnetization is known to decrease faster than that of TM sublattices [35–37]. Accordingly, when $|\mu_{Er}| = |\Sigma(\mu_{Fe}) + \Sigma(\mu_{Mn}) + \Sigma(\mu_{Co})$, a compensation point appears (T_{comp}) on the magnetization trace. This occurs for the three Co-substituted compounds for which Co shares a smaller magnetic moment, but the Co–Co and Co–Fe exchange interactions are known to increase markedly. The substitution of Co to Mn or Fe induces noticeable changes in the magnetic characteristics, as shown Figure 3. T_C increases from 355 K for $Er(Fe_{0.8}Mn_{0.2})_2$ to 550, 475, and 555 K for $Er(Fe_{0.8}Mn_{0.1})_2$, $Er(Fe_{0.7}Mn_{0.2}Co_{0.1})_2$, and $Er(Fe_{0.7}Mn_{0.1}Co_{0.2})_2$, respectively, and in all cases a compensation point $T_{comp.}$ is observed close to 450 K.

For all compounds, 5 K-isothermal magnetization traces measured in magnetic fields ranging from 0 to 7 T are shown in Figure 4. Please recall the equivalence of units emu/g (CGS) ≡ Am^2/kg (SI).

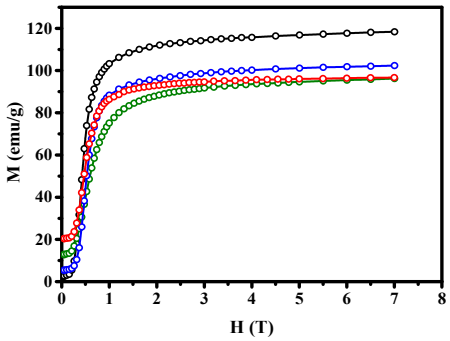

Figure 4. Magnetization traces at 5K of $Er(Fe_{0.2}Mn_{0.8})_2$ (black), $Er(Fe_{0.8}Mn_{0.1}Co_{0.1})_2$ (green), $Er(Fe_{0.7}Mn_{0.2}Co_{0.1})_2$ (blue), and $Er(Fe_{0.7}Mn_{0.1}Co_{0.2})_2$ (red) upon increasing the applied field up to 7 T.

The net magnetization increases rapidly for applied fields lower than 1 T and then evolves almost linearly for H > 1.5 T. An approach to saturation magnetization was expressed fitting the 5 K magnetization traces [38]:

$$M(H) = M_{sat} - \frac{a}{H} \quad (1)$$

with *a* being a phenomenology parameter.

Table 2 reports the saturation magnetization values of the samples. One can see that M_{sat} decreases from 6.01 μ_B for $Er(Fe_{0.8}Mn_{0.2})_2$ to 4.93, 5.26, and 5.00 μ_B for $Er(Fe_{0.8}Mn_{0.1}Co_{0.1})_2$, $Er(Fe_{0.7}Mn_{0.2}Co_{0.1})_2$, and $Er(Fe_{0.7}Mn_{0.1}Co_{0.2})_2$. Estimates of the mean <TM> magnetic moments reported in Table 2 were simply derived as $M_{TM} = (M_{Er} - M_{sat})/2$, with respect to free ion value of ~9 μ_B attributed to the Er moment [38,39].

Table 2. Total magnetic moments and TM moments for $Er(Fe_{0.8}Mn_{0.2})_2$, $Er(Fe_{0.8}Mn_{0.1}Co_{0.1})_2$, $Er(Fe_{0.7}Mn_{0.2}Co_{0.1})_2$, and $Er(Fe_{0.7}Mn_{0.1}Co_{0.2})_2$ compounds at 5 K.

Compounds		Molar Mass (g/mol.)	M_{sat} (emu/g)	M_{sat} (μ_B/f.u.)	$<\mu_{3d}>$ (μ_B/f.u.)
$Er(Fe_{0.8}Mn_{0.2})_2$	1	278.586	122.38	6.10	1.45
$Er(Fe_{0.8}Mn_{0.1}Co_{0.1})_2$	2	279.385	100.04	5.00	2.00
$Er(Fe_{0.7}Mn_{0.2}Co_{0.1})_2$	3	279.204	105.23	5.26	1.87
$Er(Fe_{0.7}Mn_{0.1}Co_{0.2})_2$	4	280.003	98.41	4.93	2.04

In a first attempt to derive each of the TM contributions to the overall <TM> magnetization, we have considered the <TM> values both expressed from the 1–2 and 3–4 formula differences (as numbered in Table 2), assuming μ_{Er} and μ_{Fe} almost constant. For these differences, the $|\mu_{Mn} - \mu_{Co}|$ values are found of 5.5 and 1.65 μ_B, respectively.

Accordingly, markedly different (or unrealistic) results suggest that, in these series of $Er(Fe\text{-}Mn\text{-}Co)_2$ compounds, some of the TM moments are far to exhibit determined values. Howbeit, the values estimated from magnetic saturation approach should be as well questioned. Otherwise, it was considered that the anisotropic magnetic hyperfine interaction at the Fe(TM) nuclei should play a role on the magnetic polarization level and orientation of the Fe(TM) moment in the RFe_2 binaries [39]. However, in most RFe_2 and particularly in the $ErFe_2$, the Fe moment was shown to behave almost smoothly as early reported e.g., in [20,21,30,31,35–41]. Back to the values that were received from saturation magnetization measurements undertaken on the simple $Er(Co_{1-x}Fe_x)_2$ system [28], the Fe and Co moments were found to be equal to 1.97 and 1.47 μ_B, respectively. For the border compositions, one can remark that the Fe and Co moments undergo an exact reduction of 0.22 μ_B reference to their 3d metal values. Moreover, for the intermediate composition $Er(Co_{0.875}Fe_{0.125})_2$ the mean $<\mu_{TM}>$ value of 1.54 μ_B fairly corresponds to the Co/Fe ratio contributions. Accordingly, it should be anticipated that, here, the Mn moment support most of the TM magnetization dispersion in the four studied compounds. More fundamental analyses devoted to the magnetic characteristics of the $R(TM)_2$ compounds of C15 type with TM = Mn, Fe, and Co, lead to, concluding that, in R-Mn binaries as well as many Mn based intermetallics, low-temperature magnetic instabilities are related to trends for antiferromagnetic ordering [42,43]. Often, both the 4f–3d and 3d–3d interactions are negative leading either to complex non-collinear magnetic structures, or weakening the (even no) local magnetic moment as for $Tb_{1-x}Y_xMn_2$ [42], $Y(Fe_{1-x}Mn_x)_2$ [43], Th_6Mn_{23} [44–46], $(Fe_{1-x}Mn_x)B$ [40] This is especially the case for structures sharing a CN12 tetrahedral-close-compact TM network (based on Friauf-polyhedra or cuboctahedra).

Conversely, the mean moment of the TM site increases when Co is substituted to Mn. If at low temperature in the binary RCo_2, cobalt exhibits band paramagnetism, it is promptly polarized by internal or external fields, as mentioned in ref. [41]. Subsequently, according to the generalized Slater-Pauling chart, the magnetic moment shared by the TM lattice increases with the Co content [38]. Assuming for μ_{Fe} and μ_{Co} almost constant values of 2.0 and 1.5 μ_B, as mentioned above, a simple evaluation based on the μ_{3d} values reported in Table 2 leads estimating roughly the μ_{Mn} values to −0.75, 2.9, 1.6, and 3.0 μ_B for $Er(Fe_{0.8}Mn_{0.2})_2$, $Er(Fe_{0.8}Mn_{0.1}Co_{0.1})_2$, $Er(Fe_{0.7}Mn_{0.2}Co_{0.1})_2$, and $Er(Fe_{0.7}Mn_{0.1}Co_{0.2})_2$, respectively. This means that, in the Mn-richest compound, $Er(Fe_{0.8}Mn_{0.2})_2$, Mn should be lower-even-negative magnetically polarized.

The molecular field picture of Curie temperature T_C of a ferrimagnetic R-TM system leads write:

$$T_C = \frac{1}{2}[T_{TM} + T_R + ((T_{TM} - T_R)^2 + 4T^2{}_{R\text{-}TM})^{1/2}] \quad (2)$$

where T_{TM}, T_R, and $T_{R\text{-}TM}$ represent the contributions to T_C due to TM-TM, R-R, and R-TM exchange interactions respectively. Reference to classical notations, the respective Curie temperature are defined from the respective C_{TM} and C_R Curie constants and molecular field coefficients $n_{TM\text{-}TM}$, $n_{R\text{-}TM}$ and $n_{R\text{-}R}$, respectively [47]. Note that $T^2{}_{R\text{-}TM}$ is proportional to the de Gennes' factor of the rare earth element with $G(J) = (g_J - 1)^2J(J + 1)$. Hence, if one considers that the $T_{R\text{-}R}$ contribution is negligible (a few % of T_{TM}) and $T_{R\text{-}TM} << T_{TM}$ [47,48] (here $n_{R\text{-}TM}$ said constant with temperature [49]), so $T_C - T_{TM}$ should be proportional to G(J). Experimentally, the Curie temperature of $ErFe_2$ is found to be approximately 10 K higher than that of $LuFe_2$ (Lu non-magnetic) of 570 K [50,51], allowing quantifies the value of de Gennes' type contribution. Subsequently, one may consider the expression (2) as a simplified following writing introducing a phenomenological coefficient:

$$T_C/T_{TM} \sim [1 + (1 - 4\alpha)^{1/2}] \quad (3)$$

Accordingly, from the μ_{TM} magnetization values derived from Table 2 and the Curie temperature values reported in Table 3, ones can establish that the ratio $T_C/(<\mu_{TM>})^2$ remains almost constant and equal to 1.35 ± 0.3 for the three Co-containing compounds, but its value is much higher (1.69) for $Er(Fe_{0.8}Mn_{0.2})_2$ the Mn-only substituted to Fe compound. Here, the coefficient must be negative, leading to conclude that, in the latter binary, the Mn-TM(Fe,Co) couplings are negative in agreement to the value of −0.75 μ_B found above. Additionally, the cell volume differences that correspond to the 2–1 and 4–3 formulas are, respectively, of 7.64 and 5.6 Å^3 for similar TM atom substitutions ($Co_{0.1}$ − $Mn_{0.1}$)/u.f. This would suggest the existence of a volume anomaly $\omega = k \cdot \mu_{Mn}^2$ [42], where k relates with the various magneto-elastic contributions.

Table 3. Transition temperature and maximum magnetic entropy change for $Er(Fe_{0.8}Mn_{0.2})_2$, $Er(Fe_{0.8}Mn_{0.1}Co_{0.1})_2$, $Er(Fe_{0.7}Mn_{0.2}Co_{0.1})_2$, and $Er(Fe_{0.7}Mn_{0.1}Co_{0.2})_2$ for a (0–5 T) field change.

Compounds		Compensation Temperature (K)	Curie Temperature T_C (K)	$-\Delta S_M$ ($J \cdot kg^{-1} \cdot K^{-1}$) $T<T_{comp}/T> T_{comp}$
$Er(Fe_{0.8}Mn_{0.2})_2$	1	no	355	2.11
$Er(Fe_{0.8}Mn_{0.1}Co_{0.1})_2$	2	435	550	1.47/0.37
$Er(Fe_{0.7}Mn_{0.2}Co_{0.1})_2$	3	445	475	1.5/0.07
$Er(Fe_{0.7}Mn_{0.1}Co_{0.2})_2$	4	425	555	1.53/0.29

Figure 5a displays the isothermal magnetization traces of $Er(Fe_{0.8}Mn_{0.2})_2$ measured under magnetic fields ranging from 0 to 5 T. When increasing the magnetic field, magnetization increases very few in the paramagnetic state ($T > T_C$), conversely in the ordered state ($T < T_C$) the magnetization traces M (H) evidence a rapid saturation above 1 T. For all Co-substituted compounds, Figure 5b–d display the isothermal magnetization traces on both sides of $T_{comp.}$ One can see that all of the compounds saturate easily for $T < T_{comp}$ insomuch as the high symmetry of the Er site makes the magneto-crystalline anisotropy of [111] axis-type, very weak [52]. As aforementioned, the compounds are ferri-magnetic with the larger Er moment oriented antiparallel to the smaller <TM> moments [15,50–52]. When increasing temperature, both the TM and Er moments decrease, but the depolarization of the Er moment is faster than the TM ones [49]. Therefore, the saturation field gradually decreases with the increasing temperature. The M(H) traces recorded above T_{comp} are shown in Figure 5b'–d' and for a given field, magnetization increases first and then decreases when temperature increases from T_{comp} up to T_C. For the $Er(Fe_{0.7}Mn_{0.2}Co_{0.1})_2$ compound, the linear shape of the traces recorded at 460 K clearly indicates that T_{comp} is close to T_C, additionally with a resulting weak magnetization level of $2\mu_{TM} - \mu_{Er}$, as shown Figure 5c'.

Subsequently, an Arrott plot-type analysis [53] is used in order to define the character of the magnetic phase transitions, as shown in Figure 6. Reference to the Banerjee's criterion, the type of magnetic transition is determined from the slope of the isotherms curves, where a negative slope corresponds to a First Order Magnetic Transition (FOMT), while a positive slope corresponds to a Second Order Magnetic Transition (SOMT). For all our compounds, the Arrott plots exhibit a positive slope confirming the SOMT character.

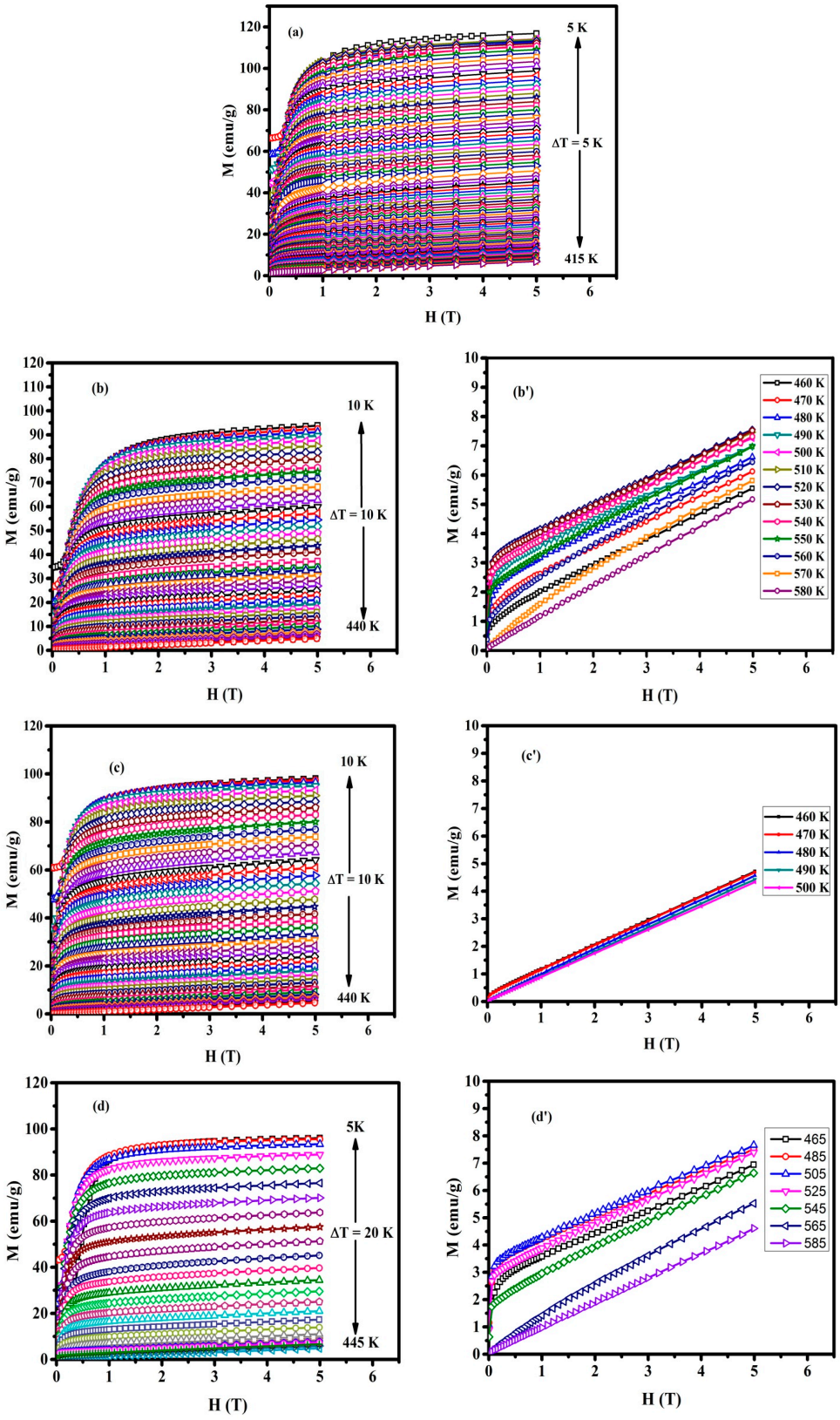

Figure 5. Variation of magnetization versus the applied magnetic field up to 5T at different temperatures for (**a**) $Er(Fe_{0.8}Mn_{0.2})_2$, (**b**,**c**,**d**) at the temperature range $T < T_{comp}$ and (**b′**,**c′**,**d′**) at $T > T_{comp}$ for $(Fe_{0.8}Mn_{0.1}Co_{0.1})_2$, $Er(Fe_{0.7}Mn_{0.2}Co_{0.1})_2$, and $Er(Fe_{0.7}Mn_{01}Co_{0.2})_2$, respectively.

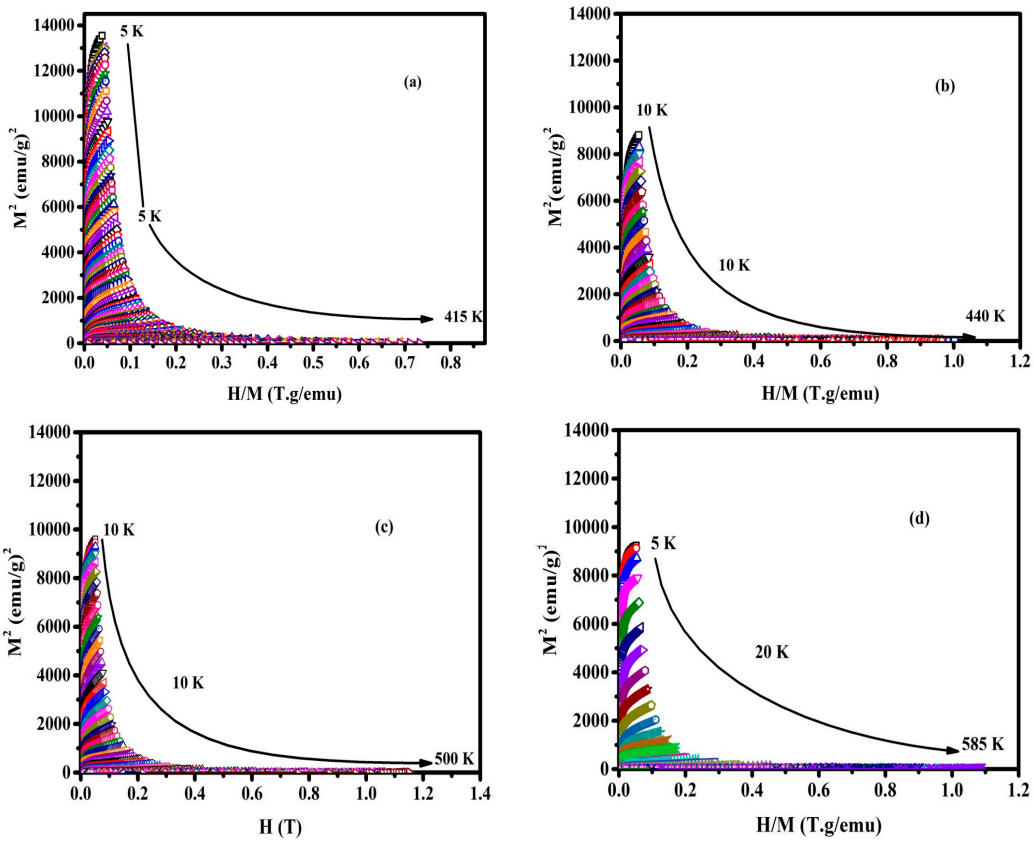

Figure 6. M^2 vs. $\mu_0 H/M$ isotherm traces plotted apart from Curie temperature for (**a**) $Er(Fe_{0.2}Mn_{0.8})_2$, (**b**) $Er(Fe_{0.8}Mn_{0.1}Co_{0.1})_2$, (**c**) $Er(Fe_{0.7}Mn_{0.2}Co_{0.1})_2$, and (**d**) $Er(Fe_{0.7}Mn_{0.1}Co_{0.2})_2$.

3.3. Magnetocaloric Properties

In a magnetization–demagnetization process, the magnetocaloric effect (MCE) is related to the change of the isothermal magnetic entropy change S_M observed when applying or removing an external magnetic field to a specific sample [54]. The magnitude of the MCE of a magnetic material is also characterized by the adiabatic temperature change ΔT_{ad} upon the magnetic field variation.

In the present work, magnetization isotherms were recorded in order to determine the total magnetic entropy change $|\Delta S_M|$ of all of the samples as a function of temperature and magnetic field change. According to the Maxwell relation, $|\Delta S_M|$ can be evaluated through the classical formula:

$$\Delta S_M(T,H) = S_M(T,H) - S_M(T,0) = \int_0^{H_{max}} \left(\frac{\partial M}{\partial T}\right)_H dH \quad (4)$$

For magnetization measured at discrete field and temperature intervals, the magnetic entropy change that is defined in Equation (4) can be approximated by Equation (5) [5,55]:

$$-\Delta S_M = \sum_i \frac{M_i - M_{i+1}}{T_{i+1} - T_i} \Delta H_i \quad (5)$$

where M_i and M_{i+1} are the experimental values of magnetization measured at temperatures T_i and T_{i+1}, respectively, under an applied magnetic field H_i.

Figure 7 shows the temperature dependence of $|\Delta S_M|$ upon a magnetic field change H = 1 to 5 T for all the studied compounds.

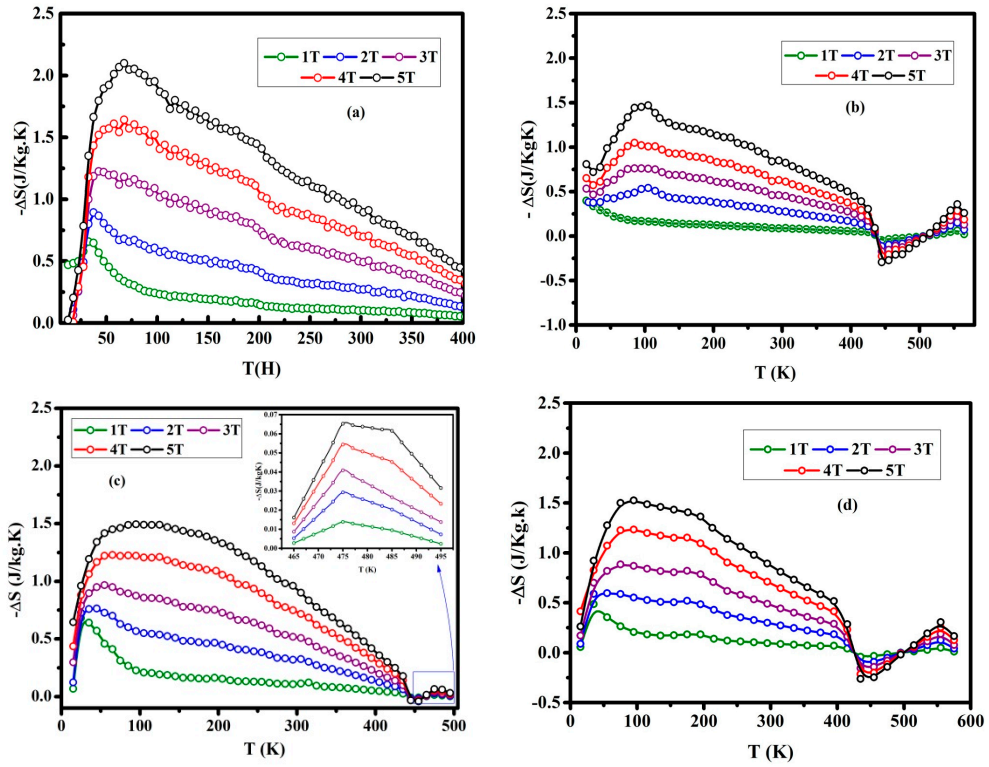

Figure 7. Magnetic entropy difference $-\Delta S_M$ versus temperature for various magnetic field shifts for (**a**) $Er(Fe_{0.2}Mn_{0.8})_2$, (**b**) $Er(Fe_{0.8}Mn_{0.1}Co_{0.1})_2$, (**c**) $Er(Fe_{0.7}Mn_{0.2}Co_{0.1})_2$, and (**d**) $Er(Fe_{0.7}Mn_{0.1}Co_{0.2})_2$. The inser of Figure 7c allows to better illustrate the thermal and field behavior of the MCE in between $T_{comp.}$ and T_C.

For all of the cases, the maximum of $|\Delta S_M|$ exhibits a linear increase when the applied maximum field is increased. As shown for $Er(Fe_{0.8}Mn_{0.2})_2$ in Figure 7a, the $|\Delta S_M|$ trace found when applying a rather weak field change of [0–1 T] mimics the susceptibility trace itself as shown on Figure 3a. But for larger magnetic field changes of [0–2 T] to [0–5 T] a wide bump of ΔS_M extends over ~400 K, making the ΔS_M (T) trace rather untypical, in comparison with classical MCE materials.

For the three Co-containing compounds, apart the first ΔS_M (T) peak setting at T_C, a second anomaly is pointed out, as shown Figure 7b–d. The latter phenomenon is related to the compensation temperature T_{Comp}. At T_C, the ΔS_M (T) value is negative as for a classical direct MCE effect, but it is positive at T_{Comp} as for a reverse MCE effect. The present phenomena fairly confirm what was found for the binary R-Fe compounds [56]. Once more, here the temperature-wide bumps of ΔS_M appear and extend over ~400 K, but are systematically ~1/3 less marked (~1.5 $J{\cdot}kg^{-1}{\cdot}K^{-1}$) than that found for $Er(Fe_{0.8}Mn_{0.2})_2$ (~2.2 $J{\cdot}kg^{-1}{\cdot}K^{-1}$) for a magnetic field change of [0–5 T]. The $\left|\Delta S_M^{max}\right|$ determinated on both side of the compensation temperature under a change of applied magnetic field of 5 T are reported in Table 3.

4. Discussion

The structural, magnetic, and magnetocaloric properties of the $Er(Fe_{0.8}Mn_{0.2})_2$, $Er(Fe_{0.8}Mn_{0.1}Co_{0.1})_2$, $Er(Fe_{0.7}Mn_{0.2}Co_{0.1})_2$, and $Er(Fe_{0.7}Mn_{0.1}Co_{0.2})_2$ compounds were investigated. The XRD results confirm that partial substitution of Co to Mn on the TM site preserves the $MgCu_2$-type structure. Around 450 K, a compensation temperature is found for the $Er(Fe_{0.8}Mn_{0.1}Co_{0.1})_2$, $Er(Fe_{0.7}Mn_{0.2}Co_{0.1})_2$ and $Er(Fe_{0.7}Mn_{0.1}Co_{0.2})_2$ compounds, involving a ferri-magnetic arrangement between the Er and TM magnetic sublattices.

However, the magnetic properties of the $Er(Fe_{1-x}TM_x)_2$ Laves phase compounds with TM = (Mn, Co) and x = 0.2 or 0.3 are not so obvious to describe and understand. Hereafter, the main characteristics

of members of cubic RTM_2 C15-type compounds will be briefly recalled, mainly focusing on the R = Er systems, with TM = Fe, Co, and Mn successively.

The bulk magnetic properties of the $ErFe_2$ binary has been well described while using a molecular field type model with negative magnetic exchange couplings in between the heavy rare earth element (e.g., Er) centering the Friauf type polyhedron formed by TM (Fe) atoms. The magnetic moments of both elements correspond almost well to the free metal values [38–40] the main coupling exchange interactions to consider are the positive Fe-Fe and the negative Er-Fe one which is addressed via the 3d–5d–4f path. As a matter of proof, hydrogen insertion to form $ErFe_2H_x$ hydrides leads to 1–a progressive decrease of the H_{hf} field transferred from the Fe sites that generates 2–a reduction of the J(Er) kinetic momentum, 3–a subsequent decrease of the 4f(Er) magnetic polarization, and 4–a weakening of the 3d(Fe)–5d(Er) overlap efficiency upon changes of conduction electron density at the Fermi level E_F via the 1s(H)–3d(Fe) hybridization. Consequently, the 3d(Fe) local moment appears slightly diminished, but a decrease of the Fe-Fe and Fe-Er exchange forces lead to a net decrease of both T_C and T_{Comp} [35,57–62]. All of these changes can be well described using a molecular field type picture.

The case of the RCo_2 binary with the C15 cubic structure was recently recalled in a recent paper that was dedicated to MCE interests [28]. In fact $ErCo_2$ is a typical example of RCo_2 compounds which magnetism is beyond the limits of Co itinerant electron meta-magnetism [58–60] leading to a 1st order magnetic ordering at T_C ~43 K only. This occurs thanks to the Er hyperfine transferred field, so, after substituting with a few amount of Fe to Co, the paramagnetic level is increased related to a Density of State (DOS) band transfer, leading to extend the magnetic ordering up to highest temperature, as we observed in ref [28].

In the R-Mn binary compounds, Mn was shown to induce very spectacular magnetic features, as e.g., for the isotypes Y_6Mn_{23}–ferromagnetic (FM with T_C ~500 K)/Th_6Mn_{23} Pauli paramagnet and $Y_6Mn_{23}H_{\sim 23}$ Pauli paramagnet/$Th_6Mn_{23}H_{23}$–FM (T_C ~350 K) [44–46,62]. It is worth to note that the R_6TM_{23} series (SG Fm3m) and the RTM_2 C15 series (SG Fd-3m) exhibit very close structure coordination features that consist in CN12 TM-coordination number of the R atom, forming a cuboctahedron for the former and a Friauf-type polyhedron for the latter. For such high coordination numbers, the formation (or loss) of a local 3d magnetic moment apart a critical Mn-Mn distance was proposed and questioned by several authors [63,64]. Effectively, the magnetic moment configurations are very different in the RMn_2 series with very low magnetic ordering transitions (e.g., ~10–30 K), evidence of several type AFM ordering, weak (<1 μ_B) or no 3d-magnetic moment [42,43,63,64]. When using interstitial hydrogen as a distance spacer the situation was observed to evolve, then the change of electron s-type density must also be accounted for [44,45,61]. In ref. [42], the nature of magnetic polarization and interactions was analyzed more systematically, aiming distinguish the model of Mn-Mn critical distance effect to d-band meta-magnetism considerations, reference to that a deep minimum of DOS should occur at E_F. Accordingly, it depends whether or not the $J_{TM\text{-}TM}$ exchange forces are positive (Co-Co), negative (Mn-Mn), or intermediate (e.g., Fe-Mn), also accounting for the $J_{R\text{-}TM}$ coupling forces.

Subsequently, several groups have questioned the magnetic characteristics of $R(TM_{1-x}TM'_x)_2$ pseudo-ternary compounds, TM,TM' ϵ{Mn, Fe, Co, Ni}. Ref [65] provides one of the more extended and recent overviews on the magnetoelastic and magnetocaloric properties of such C15 based Laves phase compounds.

Back to the more complex situation organized here with the $Er(Fe_{1-x}(Mn\text{-}Co)_x)_2$ compounds, the elementary analysis developed here tends to demonstrate that Mn could achieve very different levels and signs in its magnetic polarization up to temperatures rather high. This apparent type of meta-magnetism appears to be enhanced by both the rather robust 3d-Fe and 4f-Er magnetism, and the relative force of the exchange interactions shared by Co substitutions.

A more detailed knowledge of each particular TM element contributions seems difficult to establish more ahead either from bulk magnetization analysis or by using neutron diffraction. In fact, a non-collinear magnetic ordering, depending on the hydrogen content, has yet been proposed by using

the latter technique to characterize the magnetic structure in the $ErFe_2$-H system [66]. Besides, and very recently, meta-magnetic transitions were pointed out in the derivate parent system $Y_{1-x}Er_xFe_2(H,D)_{4.2}$ involving inversion from AFM to FM couplings in between Er and Fe lattices [67]. However, for these large hydrogen content, the cubic symmetry of the C15 crystal structure is lowered to a monoclinic space group (C2/m, even better Pc), due to a specific ordering on the tetrahedral site occupancy by H(D). So, a simple parallel teaching is not made possible to establish.

Here, the high symmetry of the 8a (Er) and 16d (TM) sites forming the Friauf coordination and the random distribution of the three TM elements lead to global information, only. Subsequently, magnetoresistance measurements and e.g., local probes, such as XMCD, ^{57}Fe (reference to the systematic work [39]), ^{57}Co and ^{166}Er Mössbauer spectroscopy, also NMR spectroscopies ... should be considered to detail the magnetic properties of the $Er(Fe_{1-x}(Co\text{-}Mn)_x)_2$ series. However, the concluding statements found in [67], as well as several refs herein mentioned, are of interest, since focusing on a meta-magnetic process is related to an itinerant electron meta-magnetic behavior of the Fe(TM) sublattice and corresponding to peculiarities (or changes) of DOS at the Fe Fermi level.

Furthermore, the very detailed work, but mainly dedicated to R-Co binaries or pseudo-binaries, could serve as reference guide [68]. Accordingly, the Spin Fluctuation Theory (SFT) [69] expressed under the Gaussian approximation [70] looks to be considered here (temperature and field dependencies, 2nd order transition). Complementary, electronic structure calculations leading to derive theoretical trends of the magnetic and elastic properties e.g., as recently reported for $TbFe_2$ and $TbCo_2$ systems in ref. [71] should be of interest to compare after using a KKR-CPA code, the present $Er(Fe_{1-x}TM_x)_2$ compounds, as well to their hydrides.

5. Conclusions

The entropy variation ΔS_M recorded on the present compounds versus a small field variation mimics rather well the magnetic susceptibility behavior versus temperature. Upon application of larger and larger magnetic field variations, the ΔS_M contribution increases almost linearly up to significant levels (−1.5 to 2.2 J/kg·K); moreover, within a large temperature range of 300 to 400 K. Even if these contributions remain modest in comparison with what is received from performant magnetocaloric compounds [1–7], but in a restricted temperature range, here the ΔS_M contributions at T_C (even at $T_{comp.}$) remain especially weak. Reference made between the Stoner and the Spin Fluctuation theories [70], only the binary $ErCo_2$ [15,72] undergoing a first order transition can be related directly to a Stoner type model [58,59]. Conversely the $Er(Fe_{1-x}TM_x)_2$ with TM = Co, Mn, are relevant for a SFT model with no marked entropy effect at the second type transition.

Even if they display rather modest performances, the present $Er(Fe_{1-x}TM_x)_2$ compounds may serve as magneto-caloric elements for cryogenic applications, as effective in a wide range of temperature. This can appear as an interesting alternative to prefer the use composites of binary RCo_2 mixtures with R = Tb, Dy, Ho, Er ... [61,72–74]. Anyway, quasi binary $R(Co_{0.88}Fe_{0.12})_2$ compounds based on the latter series were recently investigated for their peculiar characteristics down to Curie temperature [75]. High field susceptibility temperature dependence was evidenced to take place in intermediate to low temperature ranges and interpreted in terms of the "weak magnetic sublattice" model. One more, such behavior supports the interest of more systematic magnetic characterizations of the RTM_2 series of Laves type compounds, with R being a heavy rare earth metal and TM being a solution of magnetic 3d metals. Otherwise, a structure spacer, such as inserted hydrogen atoms, might be of interest to modify i.e., the DOS in the vicinity of E_F and then the magnetic couplings and configurations, as already mentioned here above [29,35,44–46,67].

Author Contributions: Conceptualization, S.O., P.d.R. and D.F.; methodology, D.F. and P.d.R.; validation, D.F.; formal analysis, I.C., S.O. and D.F.; resources, S.O. and P.d.R.; experiment & data curation, I.C., S.H.-K.; writing—original draft preparation S.O.; writing—review and editing, D.F. All authors have read and agreed to the published version of the manuscript.

Funding: This research received no external funding.

Acknowledgments: This study was supported by Faculté des Sciences de Sfax and Institut Néel, Grenoble.

Conflicts of Interest: The authors declare no conflict of interest.

References

1. Pecharsky, V.K.; Gschneidner, J.K.A. Giant Magnetocaloric Effect in $Gd_5(Si_2Ge_2)$. *Phys. Rev. Lett.* **1997**, *78*, 4494–4497. [CrossRef]
2. Fujieda, S.; Hasegawa, Y.; Fujita, A.; Fukamichi, K. Direct measurement of magnetocaloric effects in itinerant-electron metamagnets $La(Fe_xSi_{1-x})_{13}$ compounds and their hydrides. *J. Magn. Magn. Mater.* **2004**, *272*, 2365–2366. [CrossRef]
3. Tegus, O.; Brück, E.; Buschow, K.H.J.; De Boer, F.R. Transition-metal-based magnetic refrigerants for room-temperature applications. *Nature* **2002**, *415*, 150–152. [CrossRef]
4. von Ranke, P.J.; De Campos, A.; Caron, L.; Coelho, A.A.; Gama, S.; De Oliveira, N.A. Calculation of the giant magnetocaloric effect in the $MnFeP_{0.45}As_{0.55}$ compound. *Phys. Rev. B* **2004**, *70*, 094410. [CrossRef]
5. Tishin, A.M. Magnetocaloric effect: Current situation and future trends. *J. Magn. Magn. Mater.* **2007**, *316*, 351–357. [CrossRef]
6. Brück, E.; Tegus, O.; Thanh, D.; Buschow, K. Magnetocaloric refrigeration near room temperature (invited). *J. Magn. Magn. Mater.* **2007**, *310*, 2793–2799. [CrossRef]
7. Wada, H.; Tanabe, Y. Giant magnetocaloric effect of $MnAs_{1-x}Sb_x$. *Appl. Phys. Lett.* **2001**, *79*, 3302–3304. [CrossRef]
8. Han, Z.D.; Wang, D.H.; Zhang, C.; Xuan, H.C.; Gu, B.X.; Du, Y.W. Low-field inverse magnetocaloric effect in $Ni_{50-x}Mn_{39+x}Sn_{11}$ Heusler alloys. *Appl. Phys. Lett.* **2007**, *90*, 042507. [CrossRef]
9. Trung, N.T.; Zhang, L.; Caron, L.; Buschow, K.H.J.; Brück, E. Giant magnetocaloric effects by tailoring the phase transitions. *Appl. Phys. Lett.* **2010**, *96*, 172504. [CrossRef]
10. Trung, N.T.; Biharie, V.; Zhang, L.; Caron, L.; Buschow, K.H.J.; Brück, E. From single- to double-first-order magnetic phase transition in magnetocaloric $Mn_{1-x}Cr_xCoGe$ compounds. *Appl. Phys. Lett.* **2010**, *96*, 162507. [CrossRef]
11. Liu, E.; Wang, W.; Feng, L.; Zhu, W.; Li, G.; Chen, J.; Zhang, H.; Wu, G.; Jiang, C.; Xu, H.; et al. Stable magnetostructural coupling with tunable magnetoresponsive effects in hexagonal ferromagnets. *Nat. Commun.* **2012**, *3*, 873. [CrossRef] [PubMed]
12. Liu, J.; Gottschall, T.; Skokov, K.P.; Moore, J.D.; Gutfleisch, O. Giant magnetocaloric effect driven by structural transitions. *Nat. Mater.* **2012**, *11*, 620–626. [CrossRef] [PubMed]
13. Pecharsky, A.O.; Gschneidner, J.K.; Pecharsky, V.K. The giant magnetocaloric effect of optimally prepared $Gd_5Si_2Ge_2$. *J. Appl. Phys.* **2003**, *78*, 4722–4728.
14. Hu, F.-X.; Qian, X.L.; Sun, J.R.; Wang, G.J.; Zhang, X.X.; Cheng, Z.H.; Shen, B.G. Magnetic entropy change and its temperature variation in compounds $La(Fe_{1-x}Co_x)_{11.2}Si_{1.8}$. *J. Appl. Phys.* **2002**, *92*, 3620–3623. [CrossRef]
15. Wada, H.; Tomekawa, S.; Shiga, M. Magnetocaloric effect of $ErCo_2$. *J. Magn. Magn. Mater.* **1999**, *196*, 689–690. [CrossRef]
16. Nikitin, S.; Myalikgulyev, G.; Tishin, A.; Annaorazov, M.; Asatryan, K.; Tyurin, A. The magnetocaloric effect in $Fe_{49}Rh_{51}$ compound. *Phys. Lett. A* **1990**, *148*, 363–366. [CrossRef]
17. Tohei, T.; Wada, H.; Kanomata, T. Large magnetocaloric effect of $Mn_{3-x}Co_xGaC$. *J. Magn. Magn. Mater.* **2004**, *272*, E585–E586. [CrossRef]
18. Provenzano, V.; Shapiro, A.J.; Shull, R.D. Reduction of hysteresis losses in the magnetic refrigerant $Gd_5Ge_2Si_2$ by the addition of iron. *Nature* **2004**, *429*, 853–857. [CrossRef]
19. Xie, Z.G.; Geng, D.; Zhang, Z.D. Reversible room-temperature magnetocaloric effect in Mn_5PB_2. *Appl. Phys. Lett.* **2010**, *97*, 202504. [CrossRef]
20. Buschow, K.H.J.; Van Stapele, R.P. Magnetic Properties of the intermetallic compounds RFe_2. *Le J. de Phys. Colloq.* **1971**, *32*, C1-672. [CrossRef]
21. Buschow, K.H.J. Magnetic Properties of some Cubic Rare-Earth-Iron Compounds of the Type RFe_2 and $R_xY_{1-x}Fe_2$. *J. Appl. Phys.* **1970**, *41*, 4066. [CrossRef]
22. Mican, S.; Benea, D.; Mankovsky, S.; Polesya, S.; Gînscă, O.; Tetean, R. Magnetic behaviour of $Er_{1-x}Zr_xFe_2$ intermetallic compounds. *J. Physics Condens. Matter* **2013**, *25*, 466003. [CrossRef]

23. Haldar, A.; Singh, N.K.; Mudryk, Y.; Nayak, A.K.; Suresh, K.G.; Nigam, A.K.; Pecharsky, V.K. Magnetostructural transition in $Ce(Fe_{0.975}Ga_{0.025})_2$ compound. *J. Appl. Phys.* **2010**, *107*, 09E133. [CrossRef]
24. Anikin, M.S.; Tarasov, E.N.; Kudrevatykh, N.V.; Zinin, A.V. Untypical Temperature Dependence of the Magnetocaloric Effect in the $Dy(Co_{1-x}Fe_x)_2$ (x = 0.10; 0.15) Compounds. *Solid State Phenom.* **2015**, *233*, 247–250. [CrossRef]
25. Anikin, M.S.; Tarasov, E.; Kudrevatykh, N.; Osadchenko, V.; Zinin, A. About the Role of Fe-Ions in the Formation of Magnetocaloric Effect in $Ho(Co_{1-x}Fe_x)_2$ Compounds. *Acta Phys. Pol. A* **2015**, *127*, 635–637. [CrossRef]
26. Halder, M.; Yusuf, S.; Mukadam, M.D.; Shashikala, K. Magnetocaloric effect and critical behavior near the paramagnetic to ferrimagnetic phase transition temperature in $TbCo_{2-x}Fe_x$. *Phys. Rev. B* **2010**, *81*, 174402. [CrossRef]
27. Zou, J.-D.; Shen, B.-G.; Sun, J.-R. Magnetic properties and magnetocaloric effect in $TbCo_{2-x}Fe_x$ compounds. *Chin. Phys.* **2007**, *16*, 3843.
28. Chaaba, I.; Othmani, S.; Haj-Khlifa, S.; Fruchart, D.; Cheikhrouhou-Koubaa, W.; Cheikhrouhou, A.; De Rango, P. Magnetic and magnetocaloric properties of $Er(Co_{1-x}Fe_x)_2$ intermetallic compounds. *J. Magn. Magn. Mater.* **2017**, *439*, 269–276. [CrossRef]
29. Chaaba, I.; Othmani, S.; Haj-Khlifa, S.; De Rango, P.; Fruchart, D. Effect of Hydrogen on the Structure, Magnetic and Magnetocaloric Properties of Laves Phase Type-Compounds $RE(Fe_{0.25}Co_{0.75})_2H_y$ with RE = Ho and Er, y = 0.0, 3.0, 3.5. *Solid State Phenom.* **2019**, *289*, 102–107. [CrossRef]
30. Ilyushin, A.; Wallace, W. Magnetic and structural studies of rare earth-iron-manganese laves phase ternaries I. *J. Solid State Chem.* **1976**, *17*, 131–133. [CrossRef]
31. Ilyushin, A.; Wallace, W. Magnetic and structural studies of rare earth-iron-manganese laves phase ternaries II. *J. Solid State Chem.* **1976**, *17*, 373–376. [CrossRef]
32. Merches, M.; Narasimhan, K.S.V.L.; Wallace, W.E.; Ilyushin, A. Magnetic Properties of $R(Fe_{1-x}Mn_x)_2$ Compounds (R = Gd, Tb, By, Ho or Er). *AIP Conf. Proc.* **1976**, *34*, 233. [CrossRef]
33. Rodriguez-Carvajal, J. Fullprof. 2k, Version 4.6 c. *Physica B* **2002**, *55*, 192. Available online: https://scholar.google.com/citations?user=mJgatLIAAAAJ&hl=en (accessed on 4 September 2017).
34. Clementi, E.; Raimond, D.I.; Reinhardt, W.P. Atomic Screening Constants from SCF Functions II. *J. Chem. Phys.* **1967**, *47*, 1300. [CrossRef]
35. De Saxce, T.; Berthier, Y.; Fruchart, D. Magnetic and structural properties of the ternary hydride phases of $ErFe_2$. *J. Less Common Met.* **1985**, *107*, 35–43. [CrossRef]
36. Dariel, M.P.; Atzmony, U. Bulk magnetic anisotropy constants of the rare-earth iron Laves compounds. *Int. J. Magn.* **1973**, *4*, 213. Available online: www.iaea.org\T1\guilsinglrightinis\T1\guilsinglrightcollection\T1\guilsinglrightNCLCollectionStore\T1\guilsinglright_PublicPDF (accessed on 16 June 2020).
37. Bargouth, M.O.; Will, G. Neutron diffraction study of $ErFe_2$. *Le J. Phys. Colloq.* **1971**, *32*, C1-675. [CrossRef]
38. du Tremolet de Lacheisserie, E.; Gignoux, D.; Schenker, M. *Magnetism*; Grenoble Sciences: Grenoble, France, 2005; ISBN 0 387 22967 1. E-book ISBN 0 387 23062 9.
39. Bowden, G.J.; Bunbury, D.S.P.; Guimaraes, A.P. Mössbauer Studies of Iron-Rare Earth Intermetallics. *J. Appl. Phys.* **1968**, *39*, 1323. [CrossRef]
40. Wallace, W.E. Mössbauer Effect Measurements of Hyperfine Interactions in Laves Phases Containing Fe Combined with Ti, Zr, Y, and the Lanthanide Metals. *J. Chem. Phys.* **1964**, *41*, 3857. [CrossRef]
41. Burzo, E. On the magnetic properties of $Y(Fe_xCo_{1-x})_2$ compounds. *Solid State Commun.* **1978**, *25*, 825–828. [CrossRef]
42. Gaidukova, I.Y.; Dubenko, I.S.; Levitin, R.Z.; Markosyan, A.S.; Pirogov, A.N. Nature of the magnetism of the subsystem in RMn_2 compounds. *Zh. Eksp. Teor. Fiz.* **1988**, *94*, 236242.
43. Schaafsma, A.; Besnus, M.; Vincze, I.; Van Der Woude, F. Effect of Mn on the magnetic moments of Fe in intermetallic compounds. *J. Magn. Magn. Mater.* **1980**, 1149–1150. [CrossRef]
44. Malik, S.; Takeshita, T.; Wallace, W. Hydrogen induced magnetic ordering in Th_6Mn_{23}. *Solid State Commun.* **1977**, *23*, 599–602. [CrossRef]
45. Commandré, M.; Fruchart, D.; Rouault, A.; Sauvage, D.; Shoemaker, C.; Shoemaker, D. Etude par diffraction neutronique des composés $Mn_{23}Y_6Dx$. *J. Phys. Lett.* **1979**, *40*, 639–642. [CrossRef]
46. Buschow, K.H.J.; Sherwood, R.C. Magnetic properties and hydrogen absorption in rare-earth intermetallics of the type RMn_2 and R_6Mn_{23}. *J. Appl. Phys.* **1977**, *48*, 4643–4648. [CrossRef]

47. Mitchell, I.V.; Coey, J.M.D.; Givord, D.; Harris, I.R.; Hanitsch, R. *Concerted European Action on Magnets (CEAM)*; Springer Science & Business Media: New York, NY, USA, 2012; pp. 72–73.
48. Belorizky, E.; Fremy, M.A.; Gavigan, J.P.; Givord, D.; Li, H.S. Evidence in rare-earth (R)–transition metal (M) intermetallics for a systematic dependence of R-M exchange interactions on the nature of the R atom. *J. Appl. Phys.* **1987**, *61*, 3971–3973. [CrossRef]
49. Buschow, K.H.J.; de Boer, F.R. *Physics of Magnetism and Magnetic Materials*; Springer Science & Business Media: New York, NY, USA, 2007; ISBN 978-0-306-48408-7.
50. Fruchart, D.; Berthier, Y.; De Saxce, T.; Vulliet, P. Etudes structurales et magnetiques des formes cubiques et rhomboedriques $LnFe_2H_x$, Ln = Er, Tb. *J. Solid State Chem.* **1987**, *67*, 197–209. [CrossRef]
51. Pontonnier, L.; Fruchart, D.; Soubeyroux, J.; Triantafillidis, G.; Berthier, Y. Structural and magnetic behaviour of $LuFe_2H_x$. *J. Less Common Met.* **1991**, *172*, 191–197. [CrossRef]
52. Talik, E.; Kulpa, M.; Mydlarz, T.; Kusz, J.; Böhm, H. Magnetic properties of $ErMn_2$ single crystals. *J. Alloys Compd.* **2003**, *348*, 12–17. [CrossRef]
53. Banerjee, B. On a generalised approach to first and second order magnetic transitions. *Phys. Lett.* **1964**, *12*, 16–17. [CrossRef]
54. Yu, B.; Gao, Q.; Zhang, B.; Meng, X.; Chen, Z. Review on research of room temperature magnetic refrigeration. *Int. J. Refrig.* **2003**, *26*, 622–636. [CrossRef]
55. Gschneidner, K.A.; Pecharsky, V.K. Magnetocaloric Materials. *Annu. Rev. Mater. Res.* **2000**, *30*, 387–429. [CrossRef]
56. Nikitin, S.A.; Talalaeva, E.V.; Chernikova, L.A.; Andreenko, A.S. Magnetocaloric effects in rare-earth magnetic materials. *Zh. Eksp. Teor. Fiz.* **1973**, *65*, 2058.
57. Rhyne, J.J.; Sankar, S.G.; Wallace, W.E. Sublattice magnetization of $ErFe_2$—H. In *Rare Earths in Modern Science and Technology*; McCarthy, G.J., Rhyne, J.J., Eds.; Plenum Press: New York, NY, USA, 1978; ISBN 978-1-4613-3054-7.
58. Cyrot, M.; Gignoux, D.; Givord, F.; Lavagna, M. Magnetism of the rare earth, 3d–Theoretical review. *J. Phys. Colloq.* **1979**, *40*, C5-171. [CrossRef]
59. Cyrot, M.; Lavagna, M. Density of states and magnetic properties of the rare-earth compounds RFe_2, RCo_2 and RNi_2. *J. Phys.* **1979**, *40*, 763–771. [CrossRef]
60. Khmelevskyi, S.; Mohn, P. The order of the magnetic phase transitions in RCo_2 (R = rare earth) intermetallic compounds. *J. Phys. Condens. Matter* **2000**, *12*, 9453–9464. [CrossRef]
61. Balli, M.; Fruchart, D.; Gignoux, D. Magnetic behaviour and experimental study of the magnetocaloric effect in the pseudobinary Laves phase $Er_{1-x}Dy_xCo_2$. *J. Alloy. Compd.* **2011**, *509*, 3907–3912. [CrossRef]
62. Wallace, W.E.; Malik, S.K.; Takeshita, T.; Sankar, S.G.; Gualtieri, D.M. Magnetic properties of hydrides of the rare earths and rare earth intermetallics. *J. Appl. Phys.* **1978**, *49*, 1486–1491. [CrossRef]
63. Hardman, K. Site magnetization of cubic and hexagonal $HoMn_2$. *J. Appl. Phys.* **1982**, *53*, 1944. [CrossRef]
64. Shiga, M. Magnetic ordering and frustration in itinerant systems: RMn_2. *J. Magn. Mag. Mat.* **1994**, *4*, 17.
65. Терёшина, И.; Cwik, J.; Tereshina, E.; Politova, G.A.; Burkhanov, G.; Chzhan, V.; Ilyushin, A.; Miller, M.; Zaleski, A.; Nenkov, K.; et al. Multifunctional Phenomena in Rare-Earth Intermetallic Compounds With a Laves Phase Structure: Giant Magnetostriction and Magnetocaloric Effect. *IEEE Trans. Magn.* **2014**, *50*, 1–4. [CrossRef]
66. Shashikala, K.; Raj, P.; Sathyamoorthy, A.; Rao, T.V.C.; Siruguri, V.; Paranjpe, S.K. $ErFe_2$–H_2 system. II. Non-collinear magnetic ordering. *Philos. Mag. B* **1999**, *79*, 1195–1203. [CrossRef]
67. Paul-Boncour, V.; Isnard, O.; Shtender, V.; Skourski, Y.; Guillot, M. Origin of the metamagnetic transitions in $Y_{1-x}Er_xFe_2(H,D)_{4.2}$ compounds. *J. Magn. Magn. Mater.* **2020**, *512*, 167018. [CrossRef]
68. Duc, N.H.; Brommers, P.E. Aspects of Rare Earth-Transition metal Intermetallics. In *Advanced Magnetism and Magnetic Materials—Volume 1*; Duc, N.H., Ed.; Vietnam National University Press: Ho Chi Minh City, Vietnam, 2014; ISBN 978-604-62-4371-7.
69. Moriya, T. Developments of the theory of spin fluctuations and spin fluctuation-induced superconductivity. *Proc. Jpn. Acad. Ser. B* **2006**, *82*, 1–16. [CrossRef] [PubMed]
70. Melnikov, N.B.; Reser, B.I.; Grebennikov, V. Spin-fluctuation theory beyond Gaussian approximation. *J. Phys. A Math. Theor.* **2010**, *43*, 195004. [CrossRef]

71. Bentouaf, A.; Mebsout, R.; Rached, H.; Amari, S.; Reshak, A.H.; Aissa, B. Theoretical investigation of the structural, electronic, magnetic and elastic properties of binary cubic C15-Laves phases TbX_2 (X = Co and Fe). *J. Alloy. Compd.* **2016**, *689*, 885–893. [CrossRef]
72. Duc, N.; Anh, D.K.; Brommer, P. Metamagnetism, giant magnetoresistance and magnetocaloric effects in RCo_2-based compounds in the vicinity of the Curie temperature. *Phys. B Condens. Matter* **2002**, *319*, 1–8. [CrossRef]
73. Valiev, E. Entropy and magnetocaloric effect in ferrimagnets RCo_2. *J. Exp. Theor. Phys.* **2017**, *124*, 968–974. [CrossRef]
74. Balli, M.; Fruchart, D.; Gignoux, D. A study of magnetism and magnetocaloric effect in $Ho_{1-x}Tb_xCo_2$ compounds. *J. Magn. Mag. Mat.* **2007**, *314*, 16–20. [CrossRef]
75. Anikin, M.S.; Tarasov, E.N.; Kudrevatykh, N.V.; Volegov, A.S.; Zinin, A.V. Magnetic properties of $R(Co_{0.88}Fe_{0.12})_2$ quasi-biany compounds. *J. Phys. Conf. Ser.* **2019**, *1389*, 012061. [CrossRef]